THE ASTROPHYSICAL JOURNAL, 350:L37–L40, 1990 February 20

X-RAY SPECTRAL SIGNATURES OF PHOTOIONIZED PLASMAS

DUANE A. LIEDAHL AND STEVEN M. KAHN
Department of Physics and Space Sciences Laboratory, University of California, Berkeley
AND
ALBERT L. OSTERHELD AND WILLIAM H. GOLDSTEIN
Lawrence Livermore National Laboratory
Received 1989 September 13; accepted 1989 December 1

ABSTRACT

Plasma emission codes have become a standard tool for the analysis of spectroscopic data from cosmic X-ray sources. However, the assumption of collisional equilibrium, typically invoked in these codes, renders them inapplicable to many important astrophysical situations, particularly those involving X-ray photoionized nebulae. We illustrate this point by comparing model spectra which have been calculated under conditions appropriate to both coronal plasmas and X-ray photoionized plasmas. We show that the (3*s*–2*p*)/(3*d*–2*p*) line ratios in the Fe L-shell spectrum can be used to effectively discriminate between these two cases. This diagnostic will be especially useful for data analysis associated with *AXAF* and *XMM*, which will carry spectroscopic instrumentation with sufficient sensitivity and resolution to identify X-ray photoionized nebulae in a wide range of astrophysical environments.

Subject headings: atomic processes — line formation — X-rays: binaries — X-rays: spectra

I. INTRODUCTION

X-ray–emitting cosmic plasmas exist in a rich variety of physical conditions, ranging from the hot (10^7–10^8 K), tenuous (10^{-3} cm^{-3}) intracluster medium in galaxy clusters, to the relatively cool (10^4–10^5 K), dense ($>10^{11}$ cm^{-3}) regions of accretion flows in X-ray binaries. Spectroscopy in the soft X-ray band (5–45 Å), which includes the K-shell transitions of C, N, O, Ne, S, and Si, and the L-shell transitions of Fe and Ni, provides a valuable probe of the extreme environments associated with these sources. However, the rather modest sensitivity and spectral resolution of the available instrumentation in this wavelength region have precluded detailed spectroscopic studies of all but a few objects. This situation can be expected to improve dramatically with the next series of major X-ray observatories (*AXAF*, *XMM*) which will provide spectroscopic data comparable in quality to that now available to solar physicists.

In terms of atomic physics processes, X-ray–emitting astrophysical plasmas divide into two broad, but sharply defined, categories, collision-dominated and photoionization-dominated. In a collision-dominated plasma, the heating is by mechanical processes, ionization is by electron-ion collisions, and excited atomic levels are populated by electron impact. The abundance peaks of soft X-ray emitting ions generally occur at temperatures greater than 10^6 K. At these high temperatures, ionization is balanced primarily by dielectronic recombination. Optically thin plasmas fulfilling these conditions are referred to as *coronal*. Coronal conditions comprise the basis of most plasma emission codes (e.g., Raymond and Smith 1977; Mewe, Gronenschild, and van den Oord 1985).

For X-ray photoionized nebulae (XPN), the presence of a strong source of ionizing radiation has a significant effect on the state of the gas. Recently, a number of models have been constructed to estimate physical conditions in such plasmas (Tarter, Tucker, and Salpeter 1969; Hatchett, Buff, and McCray 1976; Kallman and McCray 1982, hereafter KM). These calculations show that XPN plasmas are generally overionized relative to the local electron temperature. Collisional excitations out of the ground state, which involve changes in the principal quantum number, are exceptionally rare since the ratio of excitation energy to mean electron energy can be ~ 100. Instead, excited levels are populated predominantly by radiative recombination (RR) or cascade following recombination.

These differences in line excitation processes severely impair the applicability of the commonly used coronal plasma emission codes for analyzing spectra of XPN sources. The XPN calculations themselves do not include sufficient atomic detail to be used for spectral modeling. For example, individual ions are modeled in terms of representative levels, generally fewer than 10 (KM). The lack of suitable spectral models has, in fact, hampered the interpretation of the few moderate-resolution X-ray spectra of X-ray binaries (XRBs) which have so far been acquired (Vrtilek *et al.* 1986*a*, *b*).

In this *Letter*, we concentrate on the differences in line excitation mechanisms relevant to coronal and photoionized X-ray–emitting plasmas, with the aim of characterizing the degree to which these differences may be evident in the X-ray line spectra. For the XPN case, we use the solution of the ionization and energy balance equations provided by KM to obtain an estimate of the electron temperature and to set the ionization balance. We extend the KM calculations by increasing the level of detail in the atomic models for the ions Fe XVI–XIX. In order to highlight essential differences in line excitation mechanisms and the resultant spectra, we compare the XPN spectrum with the spectrum resulting from new calculations for the same ions under conditions appropriate to coronal equilibrium.

We show that the strong 3*d*–2*p* transitions which dominate Fe L-shell spectra from coronal plasmas should not be present in spectra from photoionized plasmas. Rather, the strongest lines are due to the 3*s*–2*p* transitions. This distinction may serve as an observational criterion by which X-ray sources can be classified according to the dominant mode of line excitation.

Although such classifications are qualitative, they are necessary in order to establish the context in which quantitative diagnostics are to be applied and interpreted. Indeed, even the usually straightforward task of line identification must be modified to account for the different population mechanisms operating in photoionized plasmas.

In § II, the details of the atomic calculations are discussed. We present our results concerning population mechanisms and emission rate spectra in § III. The specific mechanisms responsible for the different behavior in the two environments are discussed in some detail for select lines. In § IV, we address the problem of line identification and discuss the extent to which our results permit a classification of line-emitting plasmas into two types by virtue of their X-ray line spectra. In this *Letter*, we emphasize the qualitative aspects of our results. A more thorough treatment of Fe L-shell line formation in a wide range of physical environments will appear in a subsequent paper.

II. ATOMIC PHYSICS CALCULATIONS

Our calculations have emphasized atomic processes in highly ionized Fe since emission lines from several ionization stages of Fe are expected to be quite prominent in X-ray spectra from cosmic sources. The $n = 3$ to $n = 2$ transitions in highly ionized Fe are among the brightest soft X-ray lines seen in spectra from solar flares and active regions (see McKenzie *et al.* 1980). The supernova remnant, Puppis A, also exhibits strong Fe XVII emission (Winkler *et al.* 1981). While definitive identifications are difficult, most of the line emission which has been observed in the soft X-ray spectra from XRBs is probably due to Fe L-shell transitions (Kahn, Seward, and Chlebowski 1984; Vrtilek *et al.* 1986*a*, *b*).

We have calculated model spectra for the ions Fe XVI–XIX (sodium though oxygen isoelectronic sequences) under conditions appropriate to two distinct environments: (1) a hot coronal plasma in collisional equilibrium, and (2) an XPN. We assume ionization equilibrium (Arnaud and Rothenflug 1985) and an electron temperature of 500 eV (log $T_e = 6.76$) for the coronal spectrum and, based on the KM calculations, set the electron temperature at 10 eV (log $T_e = 5.06$) for the XPN calculation. The rate equations are solved in steady state for the excited level populations.

In both cases, we have set the electron density to 10^{11} cm^{-3}. In fact, our results are density-independent below $\sim 10^{13}$ cm^{-3}. As our calculations are fully collisional-radiative, the higher density regimes are entirely accessible. However, we limit the scope of this *Letter* in order to highlight the more salient features of line emission in XPN, deferring a treatment of the subtleties of density effects to a future paper. To further motivate our choice, it can be argued that the bulk of the X-ray line emission is unlikely to have its origin in plasmas of high density in either coronal or XPN sources. For example, the cooling times ($\propto n_e^{-1}$) implied by densities on the order of 10^{13} cm^{-3} are inconsistent with the decay times observed in solar flares (e.g., Phillips *et al.* 1982). For the case of XPN, assuming a typical XRB scale size of $\sim 10^{11}$ cm, densities above 10^{13} cm^{-3} are accompanied by the onset of nonnegligible Compton scattering opacity.

TABLE 1

CORONAL MODEL ATOMIC CONFIGURATIONS

Species	Number of Levels	Configurations
Fe XVI	242	$2s^22p^63l$, $2s^22p^53l3l'$
Fe XVII	89	$2s^22p^6$, $2s^22p^53l$, $2s^22p^54l$, $2s2p^63l$, $2s2p^64l$
Fe XVIII	113	$2s^22p^5$, $2s2p^6$, $2s^22p^43l$, $2s2p^53l$, $2p^63l$
Fe XIX	226	$2s^22p^4$, $2s2p^5$, $2p^6$, $2s^22p^33l$, $2s2p^43l$, $2p^53l$

The atomic structure, radiative decay rates, and rates for electron impact excitation have been calculated using the HULLAC atomic physics package (Klapisch 1971; Klapisch *et al.* 1977). The atomic structure is calculated using the relativistic, multiconfiguration, parametric potential method. Radiative transitions between all levels are calculated and include the multipoles $E1$, $E2$, $M1$, and $M2$. Collisional rates are calculated using the quasi-relativistic distorted wave method (Bar-Shalom, Klapisch, and Oreg 1988). The accuracy of the theoretical wavelengths and radiative rates for X-ray transitions are approximately 0.1% and 10%, respectively (Klapisch *et al.* 1977; Bar-Shalom 1989). The collisional rates agree with the predictions of previously calculated rates to within $\sim 10\%$ (Bar-Shalom, Klapisch, and Oreg 1988). Model calculations for coronal spectra have compared favorably with solar data (Liedahl *et al.* 1988).

Because of the importance of cascades following RR in an XPN, we have used larger atomic models than in the coronal case. The configurations which are included are listed in Tables 1 and 2. Collisional rates involving $n = 5$ in the Fe XVII model and $n = 4$ in the Fe XVIII and Fe XIX models have not been calculated since, at the low XPN temperature, these levels cannot be reached collisionally from their respective ground states. Furthermore, at densities likely to be encountered in astrophysical plasmas, these states will not be collisionally mixed due to the ready availability of "allowed" radiative decay channels. Further descriptions of the relevant atomic processes for the coronal case appear in Goldstein (1988) and Liedahl *et al.* (1988).

In order to test the importance of line excitation following dielectronic recombination (DR) in the XPN model, we have explicitly calculated the DR rates of Fe XVII through the Fe XVII $2s2p^66l$ channels ($l = s$, p, d, f), the lowest energy autoionizing configurations involving the $2s2p^6$ core. This calculation includes the resonant excitation of the $2s^22p_{1/2}\,2p^4_{3/2}$ level of Fe XVIII. Solution of the rate equations including these

TABLE 2

XPN MODEL ATOMIC CONFIGURATIONS

Species	Number of Levels	Configurations
Fe XVII	139	$2s^22p^6$, $2s^22p^53l$, $2s^22p^54l$, $2s2p^63l$, $2s2p^64l$, $2s^22p^55l$
Fe XVIII	198	$2s^22p^5$, $2s2p^6$, $2s^22p^43l$, $2s2p^53l$, $2p^63l$, $2s^22p^44l$
Fe XIX	341	$2s^22p^4$, $2s2p^5$, $2p^6$, $2s^22p^33l$, $2s2p^43l$, $2p^53l$, $2s^22p^34l$
Fe XX	15	$2s^22p^3$, $2s2p^4$, $2p^5$

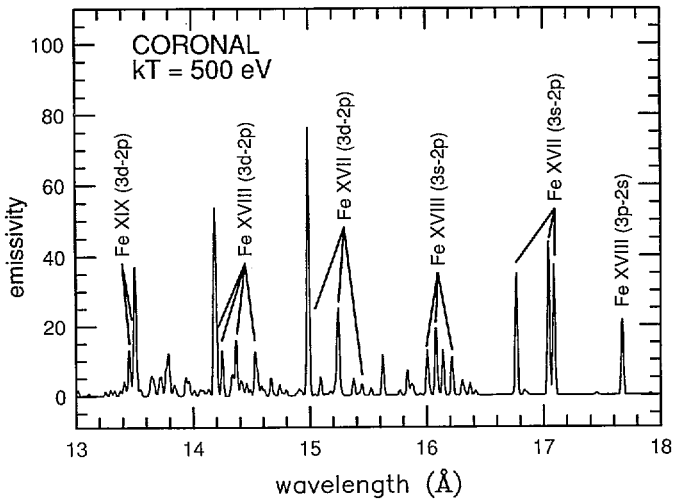

FIG. 1.—Model emission rate spectrum for Fe XVI–XIX under conditions appropriate to coronal equilibrium, $kT_e = 500$ eV, $n_e = 10^{11}$ cm^{-3}. The line profiles are Gaussian with a FWHM of 0.025 Å. The emissivity scale is arbitrary.

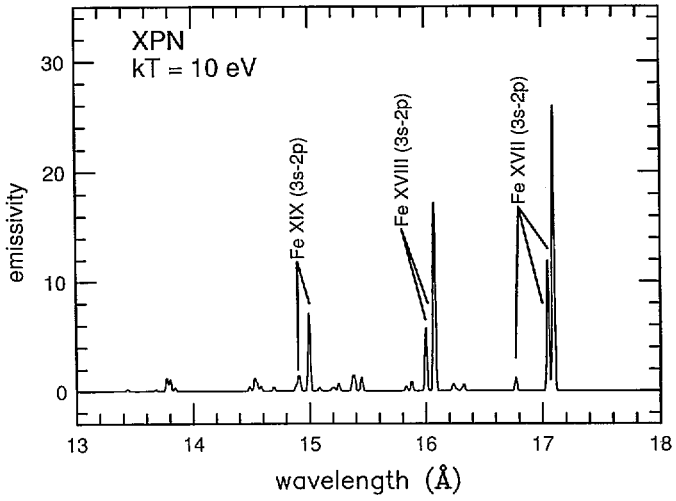

FIG. 2.—Model emission rate spectrum for Fe XVII–XIX under conditions appropriate to an X-ray–photoionized nebula, $kT_e = 10$ eV, $n_e = 10^{11}$ cm^{-3}. The line profiles and emissivity scale are the same as for Fig. 1.

processes indicates that the X-ray line spectrum is unaffected by DR of Fe XVII at low temperatures. DR through intermediate states within configurations of the form, $2s^2 2p_{1/2} 2p_{3/2}^4 nl$, can be expected to be of even less importance in light of the n^{-3} DR scaling law (Cowan 1981), since the energetics of radiationless capture requires $n > 13$. DR through higher lying doubly excited states of Fe XVII need not be considered since all autoionizing series of the form, $(2s2p)^6 nln'l'$ $(n, n' \geq 3)$ overlap a negligible fraction of the XPN electron distribution. By the same reasoning, Fe XVI DR satellites to Fe XVII resonance lines, contributors to coronal X-ray spectra (see Smith *et al.* 1985) cannot be produced in XPN. Similar arguments apply to the remaining ions in our model.

The RR cross sections are obtained from the photoionization cross sections (Scofield 1988; Saloman, Hubble, and Scofield 1988) using the Milne relation. We adopt a modified bremsstrahlung radiation field of the form $J_\epsilon = Lf_\epsilon/4\pi r^2$, where $f_\epsilon = (kT_{\rm rad})^{-1} \exp(-\epsilon/kT_{\rm rad})$. Here, ϵ is the photon energy, L is the integrated source luminosity, r is the distance from the central source, and $kT_{\rm rad}$ is the radiation temperature, taken to be 10 keV. Numerical values of L/r^2 are taken from KM.

III. RESULTS

Figures 1 and 2 show two model emission rate spectra. Figure 1 is calculated under conditions of collisional ionization equilibrium at $kT_e = 500$ eV. Figure 2 is calculated under conditions of photoionization equilibrium at $kT_e = 10$ eV. Our calculation is somewhat idealized in that we have not included line emission from other elements or higher ionization states of Fe. In the XPN case, we defer discussion of the temperature-dependent recombination continua to a future paper. Preliminary results indicate that the 13–18 Å band is not appreciably contaminated by continua. However, Fe XX lines contribute to the spectrum between 13 and 15 Å.

The model coronal spectrum shows substantial contributions from $3d$–$2p$ transitions of the Fe XVII–XIX ion stages. This is to be contrasted with the XPN spectrum which is made up almost entirely of transitions of the type $3s$–$2p$. We note, in particular, the relative strength of the Fe XVIII line blend at 16 Å in the XPN spectrum, the persistence of the Fe XVII lines at 17 Å, and the near disappearance of the Fe XVII lines at 15.01 Å and 16.77 Å in the XPN spectrum. Note that the XPN emission at ~15 Å is due to Fe XIX rather than Fe XVII. Here we will offer only brief explanations of most of these features. However, due to the "benchmark" status of the Fe XVII line at 15.01 Å, we discuss its disappearance in some detail.

The three $3d$ $(j = 1)$–$2p$ lines at 15.01, 15.26, and 15.45 Å, referred to as the C, D, and E lines (Parkinson 1973), and the three $3s$–$2p$ lines at 16.77, 17.05, and 17.10 Å, the F, G, and M2 lines, are well-known components of solar X-ray spectra. They have been the subjects of detailed studies at high temperatures, both experimentally (see Rugge and McKenzie 1985) and theoretically (see Smith *et al.* 1985). We extend this work by considering the relevant atomic process in a low-temperature, overionized plasma.

The disappearance of the $3d$ lines in the XPN emission rate spectrum is easy to understand in the context of a photoionization-dominated plasma. Due to the vanishingly small collisional rates to $3d$ states from the Fe XVII ground state, the mechanism responsible for the high intensity of these lines in coronal plasmas is inoperative in the XPN. As a result, both the $3s$ and the $3d$ states are populated by cascade following RR. The large (>25) $3s/3d$ line ratios are to be expected by virtue of the relative energies of the $3s$ and $3d$ levels, as we now explain. Since the three Fe XVII $3d$ $(j = 1)$ states have large transition rates to the ground state, they decay rapidly. The other nine $3d$ levels have $j = 0$, 2, 3, or 4 and will decay preferentially to $3p$ levels, as they have no available $E1$ channel to the $j = 0$ ground state. Thus, most of the $3d$ levels act as sources for the various $3p$ levels. Note that the majority of these latter $3d$ states are those with higher statistical weights than the levels which decay directly to the ground state. Since levels of high statistical weight receive more population influx by RR than levels of low statistical weight, the rate for populating $3p$ states by way of $3d$ states is further enhanced. At the same time, the $3p$ states, particularly the six states with $2s^2 2p_{1/2}^2 2p_{3/2}^2$ cores, are populated directly by RR. Except for the weak $E2$ lines, the $3p$ levels decay to $3s$ levels. The $3s$ population is simultaneously enhanced by direct RR into the two states with the $2s^2 2p_{1/2}^2 2p_{3/2}^3$ core. Thus, nearly all the flux into the $n = 3$ shell, whether by RR or cascades from $n > 3$, is directed to

$2s^2 2p_{1/2}^2 2p_{3/2}^2 3s$ ($j = 1, 2$), resulting in intense emission at 17.05 Å and 17.10 Å. This is not the case in coronal plasmas where much of the flux into the $n = 3$ shell originates from the ground state and goes into the $3d$ ($j = 1$) levels through electron impact excitation. Analogous behavior is seen in Fe XVIII and Fe XIX resulting in the strong line blends at 15 Å and 16 Å (see Fig. 2). Notice that the longest wavelength lines of each $3s$ series are the most intense. This behavior is a consequence of the higher statistical weights of these levels.

IV. DISCUSSION

Figures 1 and 2 show that the X-ray line spectrum can be a striking manifestation of the dominant microphysics. In particular, we have shown that the $(3s–2p)/(3d–2p)$ ratios may be used to determine the principal mode of line excitation in the highly ionized line-emitting regions of accretion-powered X-ray sources. Due to the virtual disappearance of the $3d$ lines, these ratios are of no quantitative value. However, they do provide an effective qualitative diagnostic. Additionally, ratios of $3s$ lines from different ionic species can be used to determine the ionization balance.

An example of the potential utility of the qualitative diagnostic described above is provided by the Fe XIX $3s–2p$ line just longward of 15 Å seen in Figure 2. This line could easily be mistaken for the Fe XVII $3d–2p$ line seen in Figure 1, if data were recorded with an instrument capable of only poor to moderate spectral resolution. This would lead one to conclude, following the plasma emission codes and line lists, that the temperature of the line-emitting region exceeded $\sim 2 \times 10^6$ K. Obviously, inconsistencies in the interpretation of the remaining line features would develop as a result of this faulty inference.

It is interesting to compare Figure 2 with spectral data from the low-mass XRBs, Cygnus X-2 (Vrtilek *et al.* 1986*b*), GX 9+9, and 1820−30 (Vrtilek *et al.* 1986*a*). These spectra suffer from poor statistical quality so that any conclusions, including line identifications, must be considered as tentative. However, we simply note the persistent occurrence of emission at 15 and 16 Å in these spectra. The 16 Å feature, sometimes attributed to O VIII Lyβ (Vrtilek *et al.* suggest O VIII and Fe XVIII), is accompanied by O VIII Lyα at 19 Å in spectra from coronal sources. The apparent absence of O VIII Lyα in the XRB spectra and the strength of the 16 Å feature suggest that the correct identification is the Fe XVIII line blend seen in Figure 2. As Vrtilek *et al.* (1986*a*) show for the case of GX 9+9, associating the 15 Å feature with Fe XVII emission from a hot coronal plasma is inconsistent with the strong 16 Å feature. However, if the line is identified as Fe XIX $3s–2p$, the simultaneous appearance of the 15 Å and 16 Å emission is seen to be consistent with a cool, photoionized plasma.

The high-quality data expected from future observations of astronomical X-ray sources are likely to reveal complex spectra. For example, since XRBs cannot be spatially resolved, emission originating from both coronal (e.g., White and Holt 1982) and photoionized regions may comprise their integrated line spectrum. Extraction of the relevant information concerning the geometry of XRBs and physical processes in accretion flows will rely on the successful disentanglement of such composites. The observational criterion presented here may serve as a useful discriminant in the analysis of spectroscopic data to be acquired by *AXAF* and *XMM*.

Work on this project at UC Berkeley was supported by grants from the NASA Astrophysics Data Program and the University of California Campus-Laboratory Collaborative Research Program. Work at LLNL was performed under the auspices of the US Department of Energy under contract W-7405-ENG-48. We would also like to acknowledge the Institute of Geophysics and Planetary Physics at LLNL for their extensive hospitality and for use of their computer facilities. We thank the referee for useful comments on the original manuscript.

REFERENCES

Arnaud, M., Rothenflug, R. 1985, *Astr. Ap. Suppl.*, **60**, 425.
Bar-Shalom, A. 1989, private communication.
Bar-Shalom, A., Klapisch, M., and Oreg, J. 1988, *Phys. Rev. A*, **38**, 1773.
Cowan, R. D. 1981, *The Theory of Atomic Structure and Spectra* (Berkeley: University of California Press).
Goldstein, W. H. 1988, in *IAU Colloquium 115, High-Resolution X-Ray Spectroscopy of Cosmic Plasma*, ed. P. Gorenstein and M. V. Zombeck (Cambridge: Cambridge University Press), in press.
Hatchett, S., Buff, J., and McCray, R. 1976, *Ap. J.*, **206**, 847.
Kahn, S. M., Seward, F. D., and Chlebowski, T. 1984, *Ap. J.*, **283**, 286.
Kallman, T. R., and McCray, R. 1982, *Ap. J. Suppl.*, **50**, 263 (KM).
Klapisch, M. 1971, *Comp. Phys. Comm.*, **2**, 239.
Klapisch, M., Schwab, J. L., Fraenkel, B. S., and Oreg, J. 1977, *J. Opt. Soc. Am.*, **67**, 148.
Liedahl, D. A., Kahn, S. M., Osterheld, A. L., Goldstein, W. H. 1988, in *IAU Colloquium 115, High-Resolution X-Ray Spectroscopy of Cosmic Plasma*, ed. P. Gorenstein and M. V. Zombeck (Cambridge: Cambridge University Press), in press.
McKenzie, D. L., *et al.* 1980, *Ap. J.*, **241**, 409.
Mewe, R., Gronenschild, E. H. B. M., and van den Oord, G. H. J. 1985, *Astr. Ap. Suppl.*, **62**, 197.
Parkinson, J. H. 1973, *Astr. Ap.*, **24**, 215.
Phillips, K. J. H., *et al.* 1982, *Ap. J.*, **256**, 774.
Raymond, J. C., and Smith, B. W. 1977, *Ap. J. Suppl.*, **35**, 419.
Rugge, H. R., and McKenzie, D. L. 1985, *Ap. J.*, **297**, 338.
Saloman, E. B., Hubble, J. H., and Scofield, J. H. 1988, *Atomic Data Nucl. Tables*, **38**, 1.
Scofield, J. 1988, private communication.
Smith, B. W., Raymond, J. C., Mann, J. B., and Cowan, R. D. 1985, *Ap. J.*, **298**, 898.
Tarter, C. B., Tucker, W., and Salpeter, E. E. 1969, *Ap. J.*, **156**, 943.
Vrtilek, S. D., Helfand, D. J., Halpern, J. P., Kahn, S. M., and Seward, F. D. 1986*a*, *Ap. J.*, **308**, 644.
Vrtilek, S. D., Kahn, S. M., Grindlay, J. E., Helfand, D. J., and Seward, F. D. 1986*b*, *Ap. J.*, **307**, 698.
White, N. E., and Holt, S. S. 1982, *Ap. J.*, **257**, 318.
Winkler, P. F., *et al.* 1981, *Ap. J. (Letters)*, **246**, L27.

WILLIAM H. GOLDSTEIN and ALBERT L. OSTERHELD: Lawrence Livermore National Laboratory, P.O. Box 808, Livermore, CA 94450

STEVEN M. KAHN and DUANE A. LIEDAHL: Department of Physics and Space Sciences Laboratory, University of California, Berkeley, CA 94720